STEM CELLS AND DEVELOPMENT
Volume 21, Number 6, 2012

DOI: 10.1089/scd.2010.0528

Isolation and Characterization of Human Anterior Cruciate Ligament-Derived Vascular Stem Cells

Tomoyuki Matsumoto,[1–3] Sheila M. Ingham,[1,2] Yutaka Mifune,[1–3] Aki Osawa,[1,2] Alison Logar,[1] Arvydas Usas,[1] Ryosuke Kuroda,[3] Masahiro Kurosaka,[3] Freddie H. Fu,[2] and Johnny Huard[1,2,4]

The anterior cruciate ligament (ACL) usually fails to heal after rupture mainly due to the inability of the cells within the ACL tissue to establish an adequate healing process, making graft reconstruction surgery a necessity. However, some reports have shown that there is a healing potential of ACL with primary suture repair. Although some reports showed the existence of mesenchymal stem cell-like cells in human ACL tissues, their origin still remains unclear. Recently, blood vessels have been reported to represent a rich supply of stem/progenitor cells with a characteristic expression of CD34 and CD146. In this study, we attempted to validate the hypothesis that CD34- and CD146-expressing vascular cells exist in hACL tissues, have a potential for multilineage differentiation, and are recruited to the rupture site to participate in the intrinsic healing of injured ACL. Immunohistochemistry and flow cytometry analysis of hACL tissues demonstrated that it contains significantly more CD34 and CD146-positive cells in the ACL ruptured site compared with the noninjured midsubstance. CD34+CD45− cells isolated from ACL ruptured site showed higher expansionary potentials than CD146+CD45− and CD34−CD146−CD45− cells, and displayed higher differentiation potentials into osteogenic, adipogenic, and angiogenic lineages than the other cell populations. Immunohistochemistry of fetal and adult hACL tissues demonstrated a higher number of CD34 and CD146-positive cells in the ACL septum region compared with the midsubstance. In conclusion, our findings suggest that the ACL septum region contains a population of vascular-derived stem cells that may contribute to ligament regeneration and repair at the site of rupture.

Introduction

Ligaments, made of dense connective parallel tissue fibers, play an essential role in mediating normal movement and stability of joints. Injury to these systems causes significant joint instability, which may lead to injury of other tissues and the development of degenerative joint disease. In most cases, such as with anterior cruciate ligament (ACL) [1] injury, healing fails to take place and local autograft or allograft are required to replace the native ligament. Among ligament injuries, the ACL is one of the most commonly injured structures in the knee, with approximately 100,000 ACL reconstructions performed annually in the United States alone [2]. It is well known that the ACL consists of 2 functional bundles, the anteromedial [1] and posterolateral [1] bundles [3–7]. The nomenclature of these 2 bundles is according to their insertion on the tibial footprint where the anterior medial (AM) bundle inserts anteromedially and the posterior lateral (PL) bundle inserts posterolaterally. Ferretti et al. have shown that the fetus also has a distinct ACL anatomy with 2 bundles, with a well-defined septum, constituted of vascularized connective tissue, dividing the AM and PL bundles [8].

Whereas most surgical procedures for ACL reconstruction require healing of tendon grafts in a surgically created bone tunnel, the attachment between the tendon and the bone is the weakest region in the early post-transplantation period [9,10]. In fact, it is reported that the mechanical properties of the healing ligament have not returned to normal 1 year after injury in both rabbit and canine models [11,12]. Therefore secure fixation of the tendon graft to the bone is a significant factor in allowing earlier and more aggressive rehabilitation and earlier return to sports and work. To this end, tissue engineering using stem/progenitor cells and/or growth factors with biocompatible scaffolds have recently focused on their potential for early healing and regeneration of graft tendon–bone integration [13].

Over the last decade, there has been considerable controversy about ACL intrinsic healing potential. Some surgeons

[1]Stem Cell Research Center, Children's Hospital of Pittsburgh, Pittsburgh, Pennsylvania.
[2]Department of Orthopaedic Surgery, University of Pittsburgh, Pittsburgh, Pennsylvania.
[3]Department of Orthopaedic Surgery, Kobe University Graduate School of Medicine, Kobe, Japan.
[4]Departments of Molecular Genetics and Biochemistry, and Bioengineering, University of Pittsburgh, Pittsburgh, Pennsylvania.

have reported that the ACL does not heal without reconstruction due to lack of blood clot formation, insufficient vascular supply, deficits in intrinsic cell migration, impaired growth factor ability, and effects of synovial fluid on cell morphology [14,15]. On the other hand, others have reported that the ACL spontaneously heals without surgery [16–18] or only with primary sutures [19–22]. In fact, during acute and sub-acute arthroscopic procedures for ACL reconstruction, a tibial stump is often observed and this stump can have connecting fibers to the femur and the tibia or between the posterior cruciate ligament [4] and tibia, suggesting the existence of healing potential in ACL fibers. However, there is no scientific evidence showing the healing potential in the ACL tissues. Stem cells are an attractive cell source because of their potential for high expansion, self-renewal, and multipotent differentiation capacities and could potentially be a therapeutic tool for aiding in the healing of injured ACL. Although some reports show the existence of mesenchymal stem cell-like cells [1] in human ACL tissues [23,24], their origin and characteristics still remain unclear. Recently, blood vessels have been reported to be a richer supply of stem/progenitor cells with a characteristic of expression of CD34 and CD146 surface cell markers [25–28]. Our laboratory has also identified, with molecular markers and purified by flow cytometry, 2 populations of cells that are developmentally and anatomically related to blood vessel walls in human tissues: myoendothelial cells, found in skeletal muscle and coexpressing markers of endothelial and myogenic cells (CD34 and CD56), and pericytes (positive for CD146)—also known as mural cells—which surround endothelial cells in capillaries and microvessels. These populations exhibit multilineage developmental potential and differentiate, in culture and in vivo, into skeletal myofibers, bone, cartilage, and adipocytes [28–30].

We hypothesized that CD34- and CD146-expressing vascular cells exist within the ACL tissues, especially in the septum region, and have a potential for multi-lineage differentiation and can be recruited to the site of rupture in the ACL to improve intrinsic healing.

Materials and Methods

Samples

Six ACLs were harvested from spontaneously or therapeutically aborted human fetuses that were less than 24 weeks of gestational age. The specimens were de-identified, coded, and provided by a certified Honest Broker. Human adult ACL ruptured tissues were harvested from subjects undergoing arthroscopic primary ACL reconstruction (22.5 ± 3.8 years old, 5.1 ± 1.9 months postinjury, $n = 8$). The Institutional Review Board (IRB) protocols were approved by the IRB at the University of Pittsburgh.

Hematoxylin–eosin staining

The excised fetal and adult ACL tissues were frozen in 2-methylebutane precooled in liquid nitrogen, and then stored at -80°C until they were cryosectioned. Six-micrometer sections were prepared. Hematoxylin and eosin (H&E) staining was performed for histomorphological evaluation following standard protocols ($n = 3$).

Immunohistochemical staining

The excised fetal and adult ACL tissues ($n = 3$) were frozen in 2-methylebutane precooled in liquid nitrogen, and then stored at -80°C until they were cryosectioned. Six-micrometer-thick sections were fixed in 4% paraformaldehyde for 5 min and incubated in 10% sheep serum in 2% triton-phosphate-buffered saline (PBS) for 30 min at room temperature. ACL tissues were immunostained for CD34 (stem cell marker) and CD146 (pericyte marker), coupled with α-smooth muscle actin (α-SMA) to detect various smooth muscle cells around the arterioles. Primary antibodies were purified mouse anti-human CD34 (BD Pharmingen; 1:50), and mouse anti-human CD146 (Calbiochem; 1:1,000). These were incubated for 3 h at room temperature, followed by PBS washes and incubation with secondary antibodies, anti-mouse Cy-3 (Sigma-Aldrich; 1:500) for 1 h at room temperature. FITC-conjugated anti-α-SMA (Sigma; 1:500) was added for 1 h at room temperature to detect various cells around the arterioles. Control sections were stained without the addition of the primary antibodies. Nuclei were stained with 4,6-diamidino-2-phenylindole (DAPI, Sigma; 100 ng/mL) for 5 min at room temperature. All sections were mounted with gel mount aqueous mounting medium (Sigma) and slides were observed on a Nikon Eclipse E800 (Nikon Corp.) epifluorescence microscope.

Cell isolation

The human adult ACL tissues were transported in sterile saline solution on ice. The excised ACL tissues ($n = 5$) were dissected into 2 regions, the ruptured site (Fig. 1A) and the midsubstance site (Fig. 1B). The tissues were minced into small pieces approximately 1 to 2 mm^3, washed 3 times in PBS, and then digested with 0.4% collagenase type I (0.4% w/v) (Invitrogen) in Dulbecco's modified Eagle's medium (DMEM) supplemented with 10% fetal bovine serum (FBS) and 1% penicillin/streptomycin (standard medium) for 4 to 6 h. Cells were spun down, resuspended in medium, passed through a 70-μm pore size nylon filter (BD), and washed twice with the same medium. Isolated cells from each region were cultured for 2–3 days in the standard DMEM.

Characterization of ACL-derived cells

Adult ACL-derived cells from each region were characterized by fluorescence-activated cell sorting (FACS) for

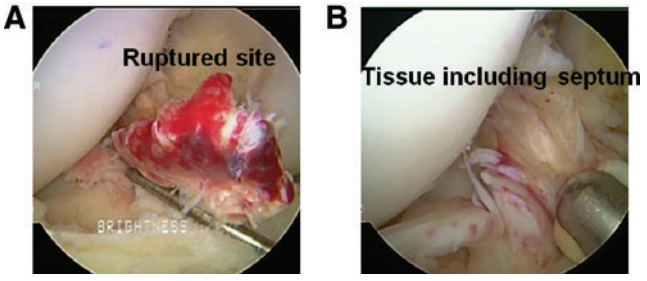

FIG. 1. Rich vascularity in the anterior cruciate ligament (ACL) tissue. Arthroscopic findings show the representative ruptured site with hematoma **(A)** and tissue including septum divided by anteromedial and posterolateral bundles **(B)**. Color images available online at www.liebertonline.com/scd

CD34 and CD146 expression. Cells were first incubated with mouse serum (Sigma; 1:10) in FACS buffer for 10 min on ice, and then were incubated with CD146-PE, CD34-APC, and CD45-FITC (BD Pharmingen) for 30 min. To exclude dead cells, 7-aminoactinomycin D (Via-probes; BD Pharmingen) was added to each tube. Live cells were analyzed using a FACS Aria Cell-Sorting System (BD) and CellQuest softwere (BD). After examining the cell marker profiles, hematopoietic cells (CD45-positive cells) were gated out and CD34+, CD146+, and CD34−CD146− cells were sorted following a protocol described by Zheng and Crisan et al. [28,29] and these 3 fractions were tested for expansion potential and multilineage differentiation capacity including osteogenesis, chondrogenesis, adipogenesis, and endotheliogenesis. In addition, CD34+, CD146+, and CD34−CD146− cells were cultured in DMEM, supplemented with 10% FBS, 10% horse serum, 1% penicillin/streptomycin, and 0.5% chick embryo extract for 2 weeks, and then were characterized by FACS for CD34, CD146, CD45, CD133, CD56, CD105, CD44, CD90, and CD73 expression. Antibodies were as follows: CD146-PE, CD34-FITC, CD45-FITC, CD133-PE, CD105-APC, CD44-PE, CD90-APC, CD73-PE, and CD56-APC (BD Pharmingen).

Assessment of expansion potential

To assess proliferation potential, CD34+, CD146+, and CD34−CD146− cells ($n=5$) were plated in 75-cm^2 collagen-coated flasks, and routine cell expansion was performed every 10 days. At each passage, cells were replated to a density of 1.0×10^5 cells/flask. The number of population doublings (PDs) for each subculturing was calculated as the $\log_2 (N/N_0)$.

Assessment of potential multilineage differentiation

Osteogenic differentiation assay. The osteogenic assay was performed as described previously ($n=5$) [31,32]. In brief, monolayer cultures of sorted cells from ACL tissues were treated with standard medium supplemented with dexamethasone (0.1 mM) (Sigma), ascorbate-2-phosphate (50 μM) (Sigma), β-glycerophosphate (10 mM) (Sigma), and bone morphogenetic protein (BMP) 4 (100 ng/mL) (Sigma) and were incubated at 37°C in 5% CO_2 for 7 days. To assess the ability to undergo osteogenesis, cells (1.0×10^5) were cultured in 6-well plates in osteogenic medium. The medium was changed every 3 days. Osteogenesis was assessed using ALP staining at day 7. Cells (2.5×10^5) were also placed in 15 mL conical polypropylene tubes and were centrifuged at 600 *g* for 5 min to establish the pellet culture assays. Pellets were cultured for 21 days in the osteogenic medium and were evaluated for their bone volume using a micro-CT (SCANCO Medical). After scanning, pellets were embedded in paraffin, sectioned, and stained with von Kossa solution for the assessment of mineralization. Total RNA was harvest on day 21 from the cells in monolayer culture with osteogenic medium. Expression of osteogenic genes collagen type IA2 (*COL I*) and osteocalcin was analyzed by reverse transcription–polymerase chain reaction (RT-PCR).

Chondrogenic differentiation assay

To assess the ability of the ACL-derived cells to undergo chondrogenesis, pellet cultures were established as described previously ($n=5$) [33–35]. Sorted cells (2.5×10^5) were placed in 15 mL conical polypropylene tubes and were centrifuged at 600 *g* for 5 min, and then were left on the bottom of the tube and cultured in chondrogenic medium (Lonza) supplemented with transforming growth factor β3 (TGF-β3) [10 ng/mL] (R&D System). After the addition of 500 μL of chondrogenic medium to each tube, the pellets were incubated at 37°C in 5% CO_2. The medium was changed every 3 days. Pellets were harvested at day 14 and their sizes were measured using ImageJ software (NIH). Paraffin-embedded pellets were assessed for chondrogenesis by Alcian blue staining at a low pH to stain the highly sulfated proteoglycans that are characteristic of cartilaginous matrix, and were counterstained with nuclear fast red, which stains cell nuclei. Total RNA was harvested from other pellets on day 21 for RT-PCR analysis. Expression of chondrogenic genes collagen type IIA2 (*COL II*) and aggrecan were analyzed by RT-PCR.

Adipogenic differentiation assay

The in vitro adipogenic assay was performed as described previously ($n=5$) [31,32]. Cells (1.0×10^5 per well) were cultured in 6-well plates for 14 days in adipogenic medium: standard medium supplemented with insulin (10 μM), dexamethasone (1 μM) (Sigma), isobutyl-methylxanthine (0.5 mM) (Sigma), and indomethacin (200 μM) (Sigma), and had the medium changed every 2 days. Adipogenesis was assessed using Oil Red O stain, which serves as an indicator of intracellular lipid accumulation. The cells were fixed for 10 min at room temperature in 10% neutral buffered formalin and then washed with PBS. They were then incubated in Oil Red O reagent for 30 min and washed with 60% isopropanol 1 time and with PBS 2 times. Total RNA was harvested for RT-PCR on day 14 from the cells in monolayer culture-maintained adipogenic medium. Expression of adipogenic genes peroxisome proliferator-activated receptor gamma (*PPARγ*) and lipoprotein lipase (*LPL*) was analyzed by RT-PCR.

Endothelial differentiation assay

The in vitro endothelial differentiation assay was performed as described previously ($n=5$) [36–39]. Cells (5.0×10^3 per well) were cultured on 24-well plates with endothelial growth medium-2 (EGM-2) Bullet kit (endothelial cell basic medium, hydrocortisone, FGF-B, vascular endothelial growth factor (VEGF), R^3-IGF-1, ascorbic acid, EGF, GA-1000, and heparin) supplemented with 10% FBS and incubated at 37°C in 5% CO_2 for 1 week. For demonstrating cellular ability to uptake 1,1′-dioctadecyl-3,3,3′,3′-tetramethylindocarbocyanine (DiI)-labeled acetylated low-density lipoprotein (acLDL) (Biomedical Technologies) and bind to *Ulex europeus* lectin (Molecular Probes), the cells were first incubated with DiI-acLDL (10 μg/mL) at 37°C for 4 h and then fixed with 1% paraformaldehyde for 10 min. After washes, the cells were continuously incubated with FITC–*Ulex europeus* lextin (10 μg/mL) for 1 h. Then, the slides were mounted by DAPI mounting medium and viewed using an inverted fluorescence microscope.

The formation of endothelial tubular structures was also studied in vitro in Matrigel cultures. Briefly, cells (1.5×10^4)

in endothelial basal medium-2 (EBM-2) were seeded onto 48-well plates coated with Matrigel (BD Biosciences). The cells were cultured at 37°C for 24 h and observed with a microscope. The total tube length was calculated from 10 randomly selected low-power fields for each experiment.

Total RNA was harvested for RT-PCR on day 7 from the cells in monolayer culture-maintained endothelial cell culture EGM-2. Expression of endothelial cell genes VE-cadherin (*VE-cad*) and *CD31* was analyzed by RT-PCR.

RNA isolation and RT-PCR

Total RNA was extracted from these cells or pellets using RNeasy plus Mini Kit (Qiagen) in accordance with the manufacture's instruction. One microgram of total RNA was used for random hexamer-primed cDNA synthesis using RT of the SuperScript II preamplification system (Invitrogen). Equal amounts of cDNA synthesis were used as templates for RT-PCR amplification per 25 μL reaction volume using Taq DNA polymerase (Invitrogen) and 50 pmol of gene-specific primers. The sequences and product sizes of primers for COL I, osteocalcin, COL II, aggrecan, PPARγ, LPL, VE-cad, CD31, and β-actin are listed in Table 1. RT-PCR amplifications were performed by preheating of the mixture at 95°C for 5 min followed by 35 cycles of 1 s at 95°C, 45 s at 58°C, and 1 s at 72°C. A final extension of 10 min was performed at 72°C. The PCR products were resolved by electrophoresis on 1.5% agarose gels and observed by ethidium bromide staining. mRNA expression of β-actin was used to normalize gene expression. Total RNA extracted from fetal cartilage, bone, fat tissues, and human umbilical vein endothelial cells was used for positive control of chondrogenic, osteogenic, adipogenic, and endotheliogenic gene expression.

Statistical analysis

The comparisons among 3 populations were made using the one-way analysis of variance. Post hoc analysis was performed by Fisher's protected least significant difference (PLSD) test. A probability value of <0.05 was considered to denote statistical significance.

Results

Vascular cells of fetal ACL

In fetal ACL tissue, there clearly exists the septum that divides the AM and PL bundles (Fig. 2A), as previously described [8]. CD34 and CD146-positive cells (red) can be seen surrounding α-SMA (green)-positive arterioles in the septum region (Fig. 2B, C). On the other hand, in the mid-substance, CD34 and CD146-positive cells were found in the region without α-SMA-positive arterioles (Fig. 2B, C).

H&E and SMA staining

H&E staining of adult ACL tissues demonstrated more blood vessel-like formation in the ruptured and septum regions than in the midsubstance region (Fig. 3A). These structures were confirmed as blood vessels by SMA staining (Fig. 3B). The number of SMA-positive cells was significantly greater in the rupture and septum regions than the mid-substance region (rupture, 205.7 ± 26.6; septum, 234.7 ± 42.8; midsubstance, $93.7 \pm 27.2/mm^2$, respectively; $P<0.05$ for rupture or septum vs. midsubstance region) (Fig. 3C).

Immunohistochemical staining and flow cytometry analysis

CD34-positive cells (red) located in α-SMA-positive arterioles (green) were abundantly found in the ruptured and septum regions compared with the midsubstance region (Fig. 3D). CD146-positive cells (red) located surrounding α-SMA (green)-positive arterioles were also found in the ruptured and septum regions compared with the midsubstance region (Fig. 3E). In the characterization of the adult ACL-derived cells by FACS analysis, the percentage of cells positive for CD34 were 46.4 ± 2.8 at the rupture site and $8.6\% \pm 0.7\%$ in the mid-substance region, and of the number of cells positive for CD146

Table 1. Primer Sequences and Product Sizes for Reverse Transcription–Polymerase Chain Reaction Analysis

Gene		*5′ DNA sequence 3′*	*Product size (bp)*
Collagen I	Forward	TGACGAGACCAAGAACTG	539
	Reverse	CCATCCAAACCACTGAAACC	
Osteocalcin	Forward	GTGCAGAGTCCAGCAAAGGT	300
	Reverse	GCAAGGGGAAGAGGAAAGAA	
Collagen II	Forward	GGCTCCCAGAACATCACCTA	198
	Reverse	ATCCTTCAGGGCAGTGTACG	
Aggrecan	Forward	TGAGTCCTCAAGCCTCCTGT	445
	Reverse	GTGCCAGATCATCACCACAC	
PPARγ	Forward	AAGACCACTCCCACTCCTTTG	554
	Reverse	TGACGAGACCAAGAACTG	
LPL	Forward	GGGCATGTTGACATTTACCC	461
	Reverse	GGCAGAGTGAATGGGATGTT	
VE-cadherin	Forward	ACGCCTCTG TCATGTACCAAA TCCT	461
	Reverse	GGCCTCGACGATGAAGCTGTATT	
CD31	Forward	ATCGATCAGTGGAACTTTGCCTATT	363
	Reverse	GTG GCA TTT GAG ATT TGA TAG A	
B-actin	Forward	CCTCGCCTTTGCCGATCC	225
	Reverse	GGAATCCTTCTGACCCATGC	

LPL, lipoprotein lipase; PPARγ, peroxisome proliferator-activated receptor gamma.

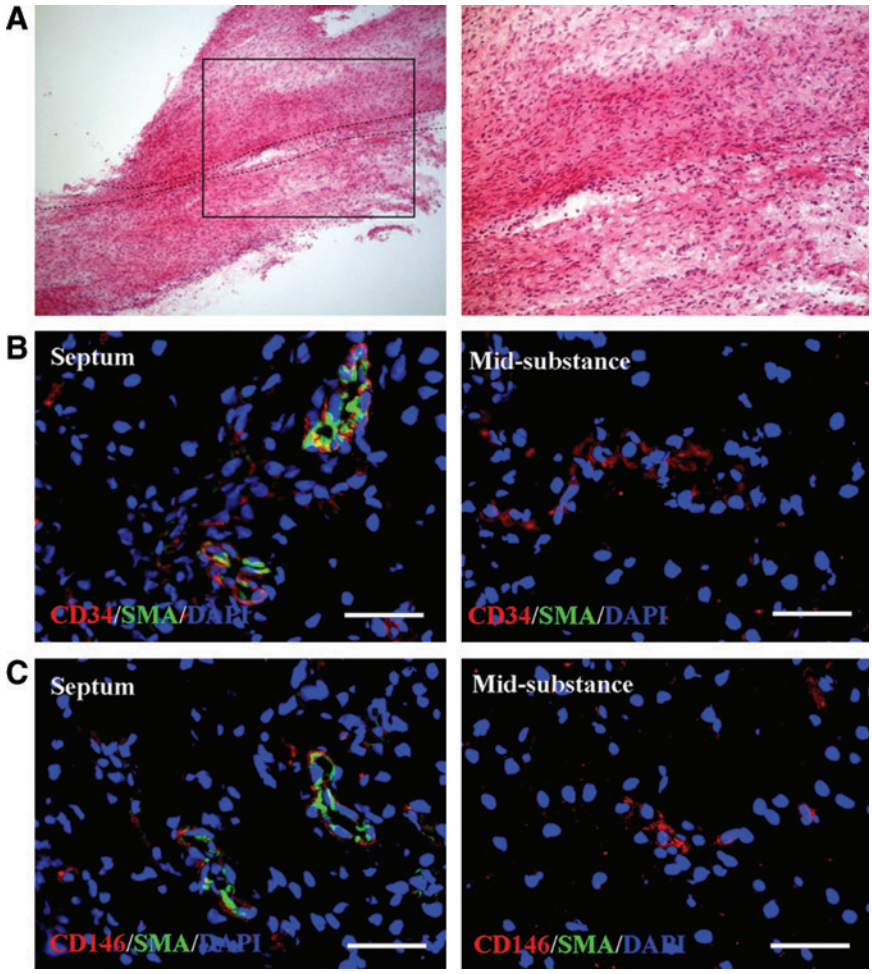

FIG. 2. Vascular cells of fetal ACL. In fetal ACL tissue, there clearly exists the septum dividing the anterior medial (AM) and PL bundles **(A)** (×100). CD34 and CD146-positive cells (red) were located surrounding α-smooth muscle actin (α-SMA) (green)-positive arterioles in the septum region **(B, C)**. In the midsubstance, CD34 and CD146-positive cells were found in the region without α-SMA-positive arterioles **(B, C)**. Scale bar: 50 μm. Color images available online at www.liebertonline.com/scd

were 7.3±2.5 at the rupture site and 1.7%±0.7% in the midsubstance region. The number of CD34+ and CD146+ cells was significantly higher at the rupture site when compared with the midsubstance region (Fig. 3F, G).

Expansion potential of adult ACL-derived cells

Adult ACL-derived cells from each region were sorted for expression of CD34 and CD146 after gating out the hematopoietic (CD45-positive cells) cells (Fig. 4A). After sorting, 6 populations (CD34+CD45−, CD146+CD45−, CD34−CD146−CD45− cells from the rupture site and midsubstance region) were cultured for 2 weeks ($n=3$ in each group). Cells from the midsubstance region did not expand well; therefore, only cells from the rupture site were analyzed for cell characterization. Interestingly, the CD34+CD45− cell fraction lost their CD34 expression and expressed CD146, CD105, CD44, CD90, and CD73 (Fig. 4B). In addition, all these cell populations showed similar patterns of cell surface marker positivity for CD146, CD105, CD44, CD90, and CD73 expression and negativity for CD45, CD133, CD56, and CD34 (Table 2) (Fig. 4C). Analysis of short-term kinetics showed that all populations had similar PD times until 3 passages; however, after moderate expansion over 4 passages, CD34+CD45− cells exhibited significantly higher PD times than the other groups in all passages ($P<0.01$ for CD34+ vs. CD146+, CD146+ vs. CD34−CD146− in passage 4–10) (Fig. 4D).

Multilineage differentiation of adult ACL cells

Osteogenic differentiation. In monolayer cultures all the population showed positive ALP staining; however, the CD34+ cells revealed a larger number of positive cells than the CD146+ cells and CD34−CD146− cells (Fig. 5A). von Kossa staining showed a greater number of positive cells in the CD34+ cell group than the other populations (Fig. 5B). Micro CT analysis showed greater mineralization in the CD34+ cell group compared with the other populations (Fig. 5C). Moreover, bone volume and density of pellets in the CD34+ cell group were significantly larger than the other populations (bone volume: CD34+, 0.84±0.03; CD146, 0.43±0.01, CD34−CD146−, 0.24±0.01 mm^3, bone density: CD34+, 288.6±21.3; CD146, 243.9±9.7, CD34−CD146−, 180.9±11.5 mg HA/ccm) (Fig. 5D). mRNA expression of COL I and osteocalcin was detected from pellets in all populations (Fig. 5E); however, the expression ratio of COL I to β-actin was significantly greater in the CD34+ and CD146+ cell populations than in the CD34−CD146− cell population (CD34+, 0.758±0.003; CD146+, 0.737±0.061; CD34−CD146−, 0.380±0.022; respectively. $P<0.01$ for CD34+ vs. CD34−CD146−, $P<0.05$ for CD146+ vs. CD34−CD146−) (Fig. 5F). The expression ratio of osteocalcin to β-actin was significantly greater in the CD34+ cell population than in the CD34−CD146− cell population (CD34+, 0.777±0.067; CD146+, 0.649±0.007; CD34−CD146−, 0.416±0.046; respectively. $P<0.05$ for CD34+ vs. CD34−CD146−) (Fig. 5F).

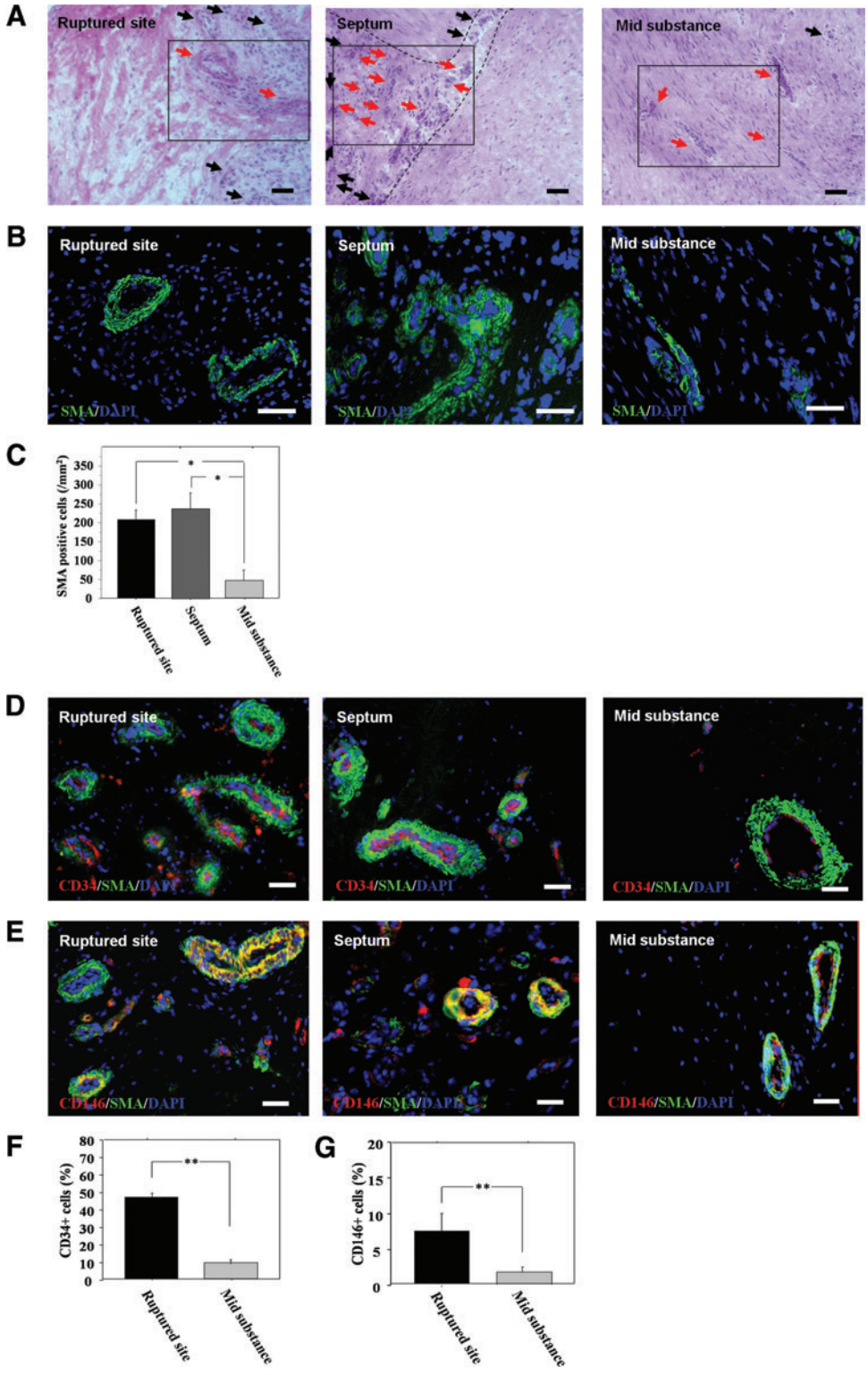

FIG. 3. **(A)** H&E staining showed more vascular-like structures in the septum and ruptured site compared with the midsubstance. *Arrow*: vascular-like structure. Scale bar: 50 μm. **(B)** α-SMA staining recognized these structures as blood vessels. Scale bar: 50 μm. **(C)** The number of α-SMA-positive cells was significantly greater in the ruptured and septum regions than the midsubstance region. $*P < 0.05$. **(D)** CD34-positive cells (*red*) located in α-SMA-positive arterioles (*green*) were abundantly found in the ruptured and septum regions compared with the midsubstance region. **(E)** CD146-positive cells (*red*) located surrounding α-SMA (*green*)-positive arterioles were also abundantly found in the ruptured and septum regions compared with the midsubstance region. **(F, G)** Fluorescence-activated cell sorting analysis demonstrated significantly higher numbers of CD34+ **(F)** and CD146+ **(G)** cells at the ruptured site compared with the midsubstance region. $**P < 0.01$. The insets in figure **A** indicate the lesion shown in Figure **B**. Color images available online at www.liebertonline.com/scd

Chondrogenic differentiation

All the populations formed pellets and their diameters were 0.72 ± 0.02, 0.79 ± 0.02, and 0.84 ± 0.05 (mm) for the CD34+, CD146+, and CD34−CD146− cells, respectively, with the CD34−CD146− cells generating significantly larger pellets than the other populations (Fig. 6A, B). Pellets generated by the CD34−CD146− cells also stained very well with Alcian blue compared with the other populations (Fig. 6C). mRNA expression of COL II and aggrecan was detected in pellets from all the populations (Fig. 6D). There were no significant differences in the expression ratio of COL II to β-actin and aggrecan to β-actin among any of the cell populations (COL II; CD34+, 0.885 ± 0.019; CD146+, 0.931 ± 0.034;

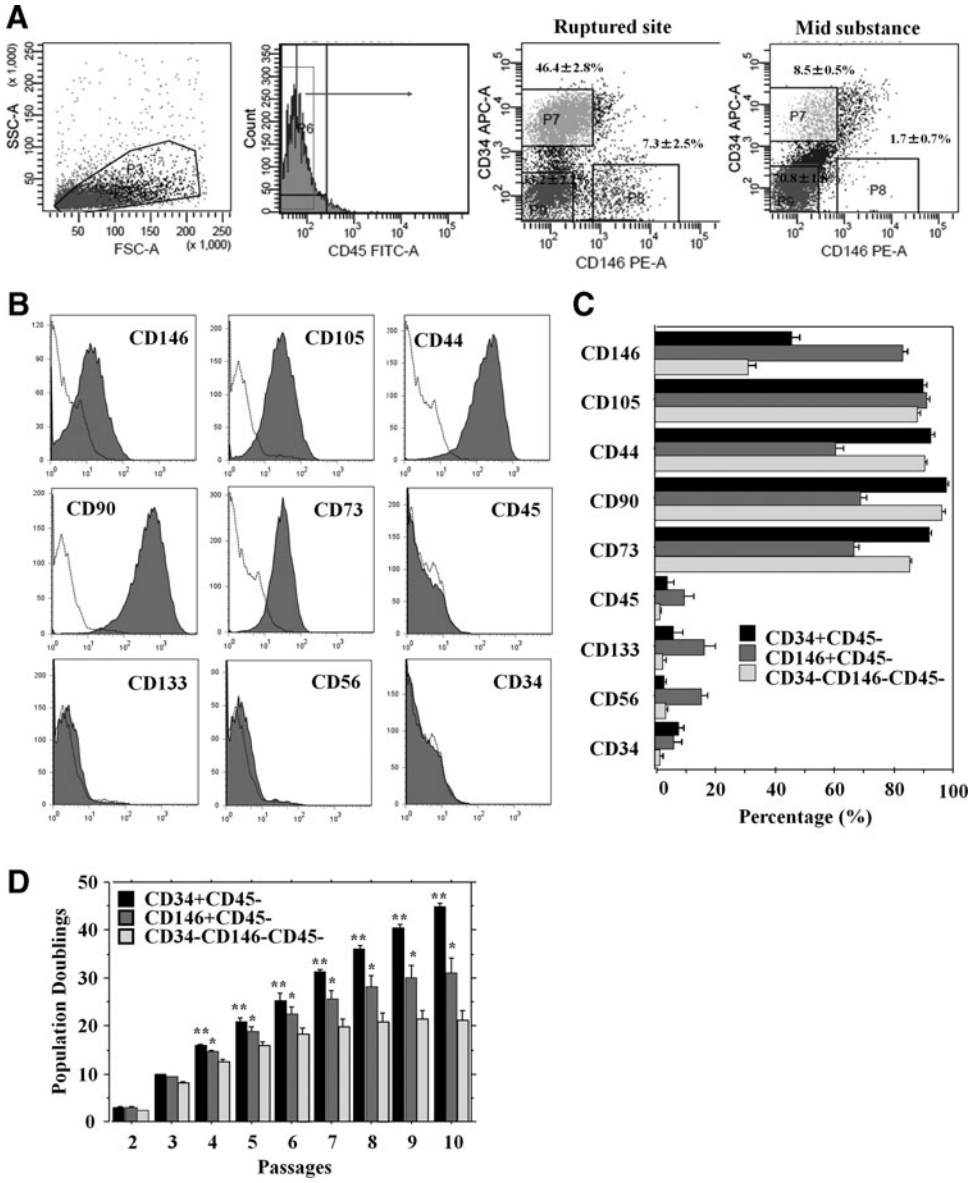

FIG. 4. (A) ACL-derived cells from the site of ACL rupture and mid-substance region were sorted for expression of CD34 and CD146 after gating out hematopoietic (CD45-positive) cells. **(B)** CD34+CD45− cell fraction lost their CD34 expression and showed positive expression for CD105, CD44, CD90, and CD73 after 2 weeks of expansion. **(C)** All these cell populations showed positive expression for CD105, CD44, CD90, and CD73 and negative expression for CD45, CD133, CD56, and CD34. **(D)** After moderate expansion over 4 passages, CD34+CD45− cells exhibited significantly higher population doublings than the other groups in all passages. $^{**}P < 0.05$ for CD34+ versus CD146+ and CD34− CD146−, $^{*}P < 0.05$ for CD146+ versus CD34−CD146−.

CD34−CD146−, 0.574±0.014. P=NS. Aggrecan; CD34+, 1.055±0.052; CD146+, 1.094±0.010; CD34−CD146−, 1.136±0.068. P=NS) (Fig. 6E).

Adipogenic differentiation

All populations were stained positively for Oil Red O (Fig. 7A). The number of Oil Red O-positive cells in CD34+, CD146+, and CD34−CD146− cells were 906.7±33.4, 816.0±36.5, and 407.1±34.6/mm^2, respectively. Oil Red O staining demonstrated that CD34+ cells had significantly more adipose cells (lipid droplets) compared with the other populations ($P < 0.01$ for CD34+ and CD146+ vs. CD34− CD146−) (Fig. 7B). mRNA expression of PPARγ and LPL was detected in all the populations (Fig. 7C). There were no significant differences, in the expression ratio of PPARγ to

Table 2. Phenotypic Characterization of Anterior Cruciate Ligament-Derived Cells by Fluorescence-Activated Cell Sorting Analysis

	(%, mean±SE)								
	CD 146	CD 105	CD 44	CD 90	CD 73	CD 45	CD 133	CD 56	CD 34
CD 34+	45.1±2.7	89.9±1.2	92.9±0.9	98.0±0.7	92.1±0.8	3.9±2.0	5.9±2.8	2.6±0.4	8.3±1.3
CD 146+	82.2±1.5	91.3±0.8	60.6±2.6	68.7±2.2	66.5±1.9	9.2±3.4	16.3±3.4	15.3±1.7	4.0±2.3
CD34−CD146−	30.7±2.9	88.1±1.1	90.9±0.3	96.6±0.6	85.2±0.8	0.9±0.6	2.2±1.0	0.8±0.5	1.3±0.6

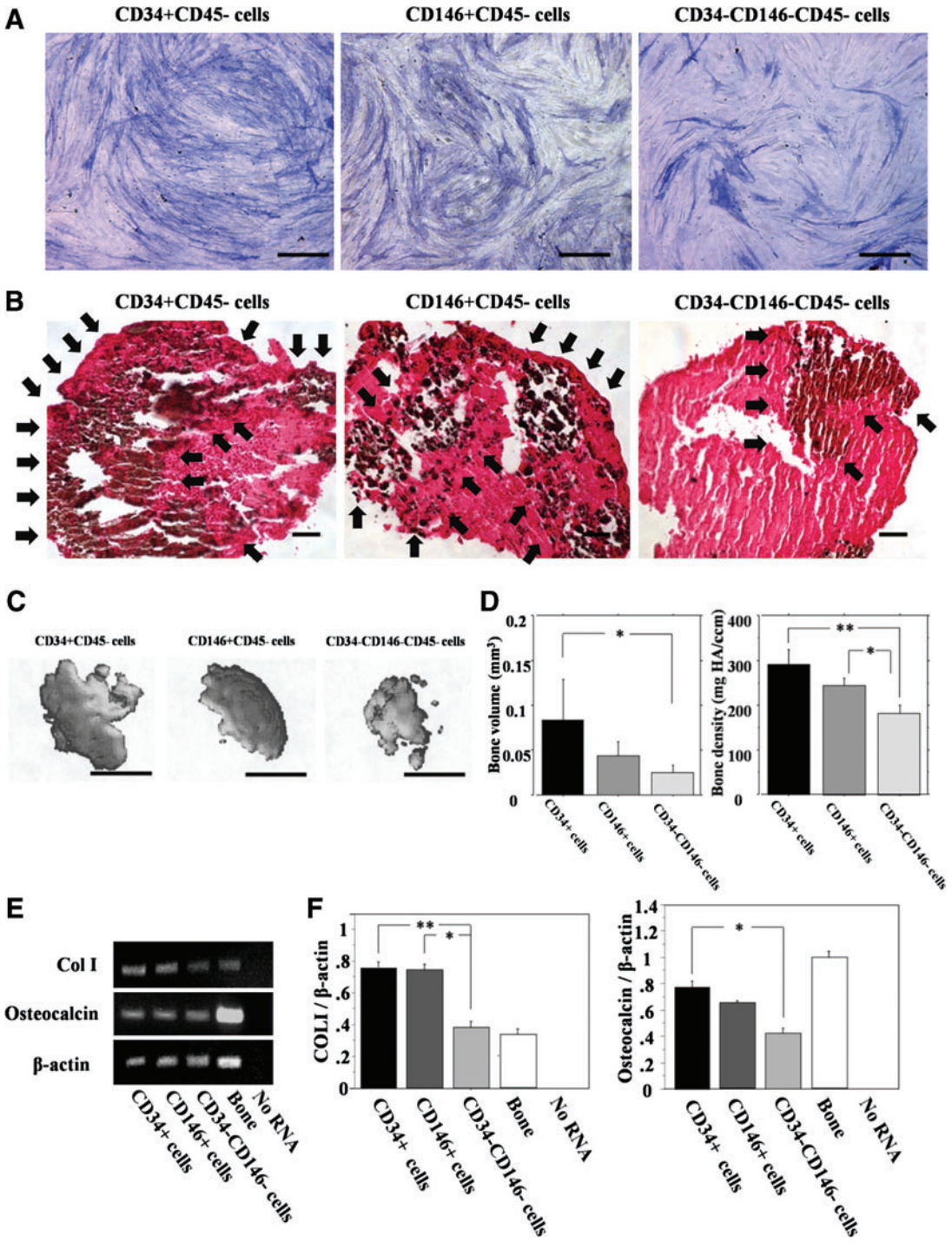

FIG. 5. **(A)** In monolayer culture, all population showed positive ALP staining; however, CD34+ cells revealed a larger number of ALP-positive cells than CD146+ cells and CD34−CD146− cells. Scale bar: 200 μm. **(B)** Mineralized nodular structures observed by von Kossa staining showed a greater number of positive cells in the CD34+ cell population than the other populations. *Arrow*: von Kossa positive. Scale bar: 200 μm. **(C)** Micro-CT analysis showed greater mineralization in the CD34+ cell population compared with the other populations. Scale bar: 500 μm. **(D)** Bone volume and density of CD34+ cells pellets were significantly larger than the other populations. $^{**}P < 0.01$, $^{*}P < 0.05$. **(E)** The mRNA expressions of collagen type IA2 (COL I) and osteocalcin were detected from pellets in all populations. **(F)** mRNA expression of COL I and osteocalcin was detected from pellets in all cell populations. The expression ratio of COL I to β-actin was significantly greater in the CD34+ and CD146+ cell populations than in the CD34−CD146− cell population. The expression ratio of osteocalcin to β-actin was significantly greater in the CD34+ cell population than in the CD34−CD146− cell population. $^{**}P < 0.01$, $^{*}P < 0.05$. Color images available online at www.liebertonline.com/scd

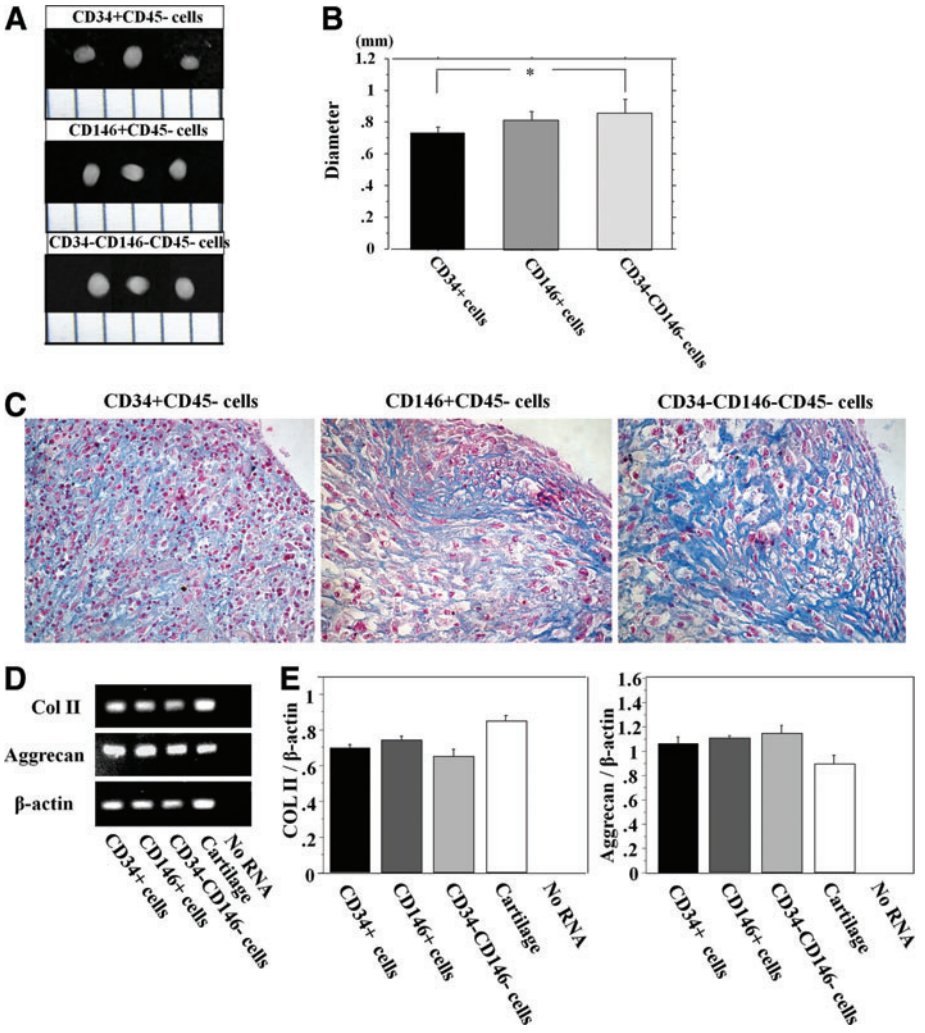

FIG. 6. **(A, B)** Although all cell populations formed pellets, CD34−CD146− cells showed significantly larger sizes than the other populations. **(C)** Pellets of CD34−CD146− cells appeared to be stained well with Alcian blue compared with the other populations. **(D)** mRNA expression of COL II and aggrecan was detected from pellets in all populations. **(E)** There were no significant differences in the expression ratio of COL II to β-actin and aggrecan to β-actin among all cell populations. *$P < 0.05$. Color images available online at www.liebertonline.com/scd

β-actin, between any of the cell populations (CD34+, 1.204 ± 0.059; CD146+, 1.120 ± 0.066; CD34−CD146−, 1.070 ± 0.046. P = NS) (Fig. 7D). The expression ratio of LPL to β-actin was significantly greater in the CD34+ and CD146+ cell populations than in the CD34−CD146− cell population (CD34+, 1.257 ± 0.068; CD146+, 1.155 ± 0.035; CD34−CD146−, 0.957 ± 0.019; respectively. $P < 0.05$ for CD34+ and CD146+ vs. CD34−CD146−) (Fig. 7D).

Endothelial differentiation

The abilities to uptake acLDL and bind to *Ulex europeus* lectin are characteristics of endothelial cells and endothelial progenitor cells (EPCs). All populations showed double-positive stainings for acLDL uptake and binding of *Ulex europeus* lectin (Fig. 8A). All populations also showed vascular tube-like structures (Fig. 8B). The tube length in CD34+, CD146+, and CD34−CD146− cells were 6.4 ± 0.6, 3.9 ± 0.9, and 1.2 ± 0.3/field, respectively. The tube formation assay demonstrated that CD34+ cells showed significantly higher potential for endothelial differentiation compared with the other populations (Fig. 8C). mRNA expression of CD31 and VE-cad was detected from all populations (Fig. 8D). There were no significant differences in the expression ratio of VE-cad to β-actin among all the cell populations (CD34+, 1.033 ± 0.008; CD146+, 0.956 ± 0.055; CD34−CD146−, 0.989 ± 0.029. P = NS) (Fig. 8E). The expression ratio of CD31 to β-actin was significantly greater in the CD34+ and CD146+ cell populations compared with the CD34−CD146− cell population (CD34+, 0.876 ± 0.071; CD146+, 0.873 ± 0.065; CD34−CD146−, 0.549 ± 0.023; respectively. $P < 0.05$ for CD34+ and CD146+ vs. CD34−CD146−) (Fig. 8E).

As control groups, we performed the each differentiation assay with each cell population: CD34+, CD146+, and CD34−CD146− with each differentiation medium not including any chemical inducers. In all results of these experiments, we could see no proof about the differentiations into all lineages, including osteogenesis, adipogenesis, chondrogenesis, and endothelial lineage in using all cell populations (data not shown).

Discussion

Initially, our study compared the characteristics of the cell populations isolated from the septum and midsubstance regions of fetal and adult ACLs. We have found that CD34 and CD146-positive cells were more prevalent in the septum region of the fetal and adult ACLs. When comparing immunohistochemical staining results of the septum region

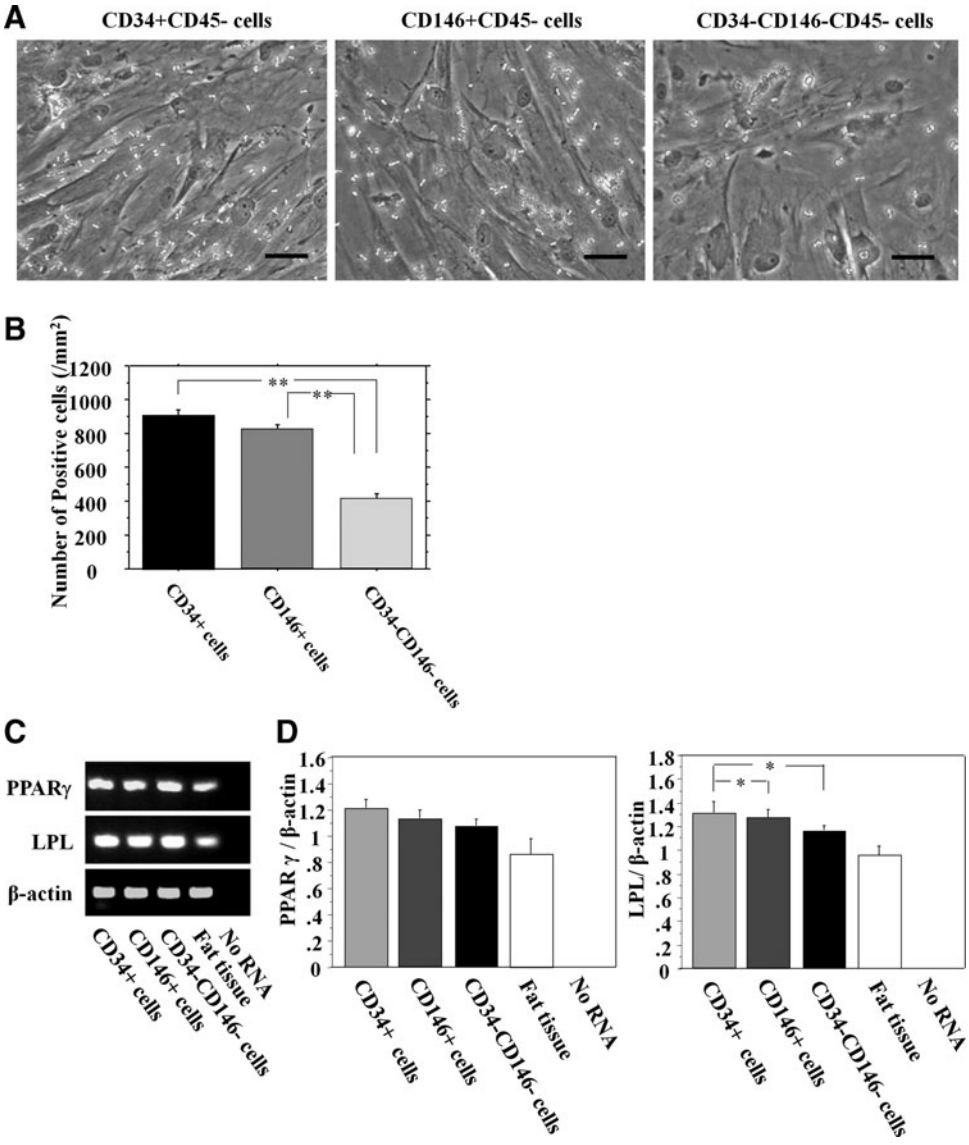

FIG. 7. (A) Although all populations were positively stained for Oil Red O. **(B)** The number of Oil Red O-positive cells demonstrated that the CD34+ cells showed significantly more adipose cells (lipid droplets) compared with the other populations. Scale bar: 100 μm. **(C)** mRNA expression of peroxisome proliferator-activated receptor gamma (PPARγ) and lipoprotein lipase (LPL) was detected in all populations. **(D)** There were no significant differences in the expression ratio of PPARγ to β-actin among all cell populations. The expression ratio of LPL to β-actin was significantly greater in the CD34+ and CD146+ cell populations than in the CD34−CD146− cell population. $^{**}P < 0.01$, $^{*}P < 0.05$.

between fetal and adult ACLs, we found a thinner capillary in the adult verses fetal septum region of the ACL. Further, the capillaries in the fetal ACL midsubstance region did not show positive α-SMA immunostaining, which might be explained by their immature stage of development. A previous embryologic study has indicated that the ACL begins to organize at the gestational age of 8 weeks and is well developed by the ninth week [40]. Gardner and O'Rahilly suggested that after embryonic developmental stage 21, the eighth week of gestational age, the ACL will continue to grow; however, no major organizational or compositional changes will occur after this point [41]. Ferretti et al. found that the vascularity of the fetal ACL was abundant, with arteries and arterioles seen during both gross and histological examination [8]. Scapinelli et al. described the neonate middle genicular artery as having a relatively greater caliber than is seen in adults and also has a longer intra-articular course [42]. Although these studies have shown the presence of an abundant vascularity in the fetal ACL, to our knowledge, no other study has characterized these vascular cells with immunohistochemistry as we have done in the current study.

As CD34-positive and CD146-positive cells were more prevalent in the septum region, the present study also compared the characteristics of the cell populations isolated from the rupture sites of an injured ACLs and the midsubstance regions of adult ACLs. CD34-positive and CD146-positive cells exhibited multilineage differentiation potential, including the capacity to undergo chondrogenesis, osteogenesis, adipogenesis, and endotheliogenesis. These findings suggest that these cell populations exhibit vascular stem cell characteristics and could contribute to primary ligament healing or tendon–bone healing after ACL reconstruction.

Our laboratory has provided evidence that the existence of myogenic cells is related to the endothelial cell lineage in human skeletal muscle, confirming that endothelial and satellite cells are closely related [29]. Covas et al. have recently shown that mesenchymal stem cells (MSCs) and pericytes are similar cell types located in the walls of the circulatory system's vasculature and function as cell sources for tissue repair and maintenance [28,43]. Reports have shown that CD34+ cells are committed not only to an endothelial cell lineage but also to mural perivascular cells

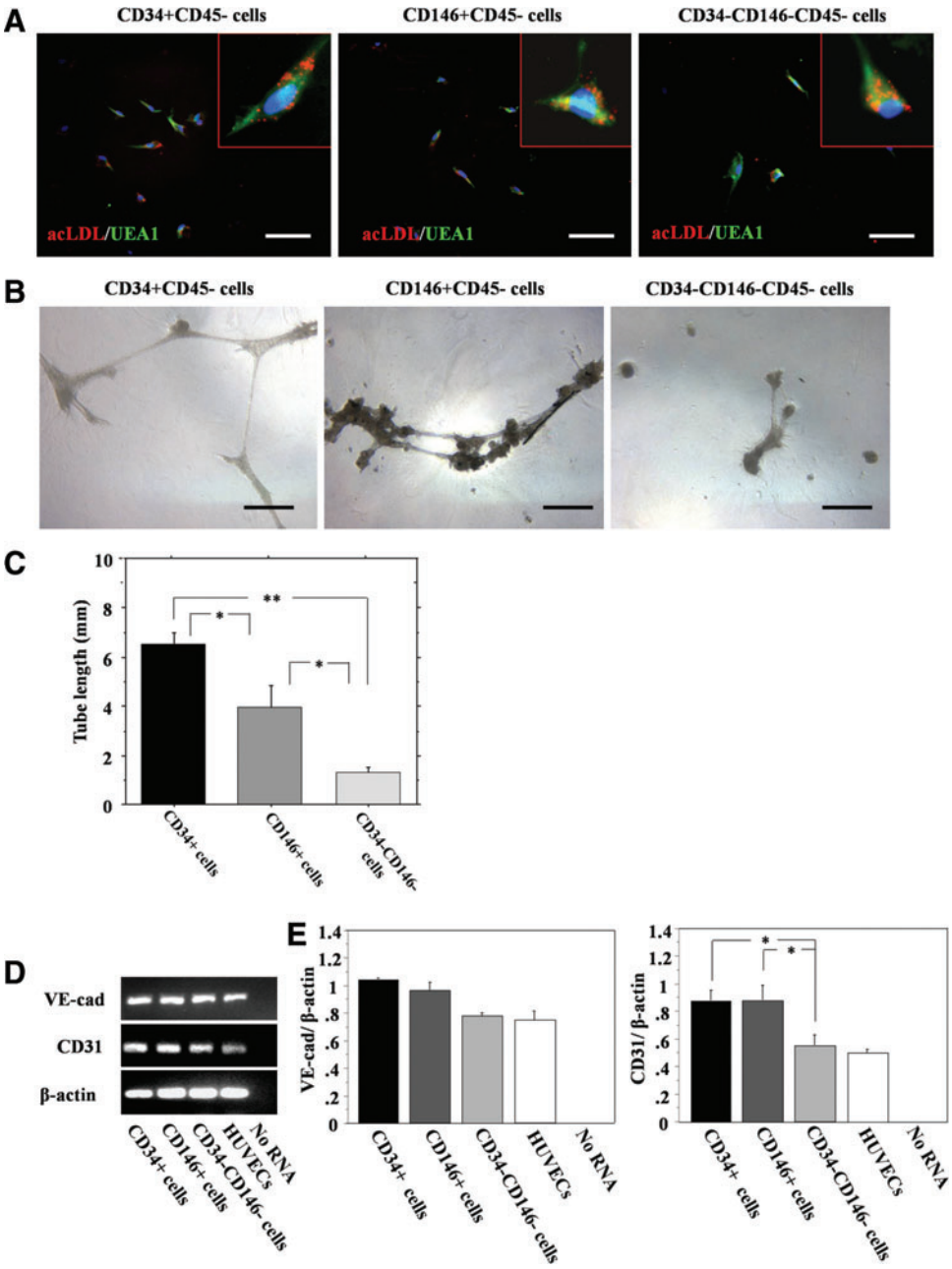

FIG. 8. **(A)** All populations showed double-positive staining for acetylated low-density lipoprotein uptake and binding of *Ulex europeus* lectin. Scale bar: 100 μm. **(B)** All populations also showed vascular tube-like structures. Scale bar: 500 μm. **(C)** Assessment of tube length demonstrated that CD34+ cells showed a significantly higher potential for endothelial differentiation compared with the other populations. **(D)** mRNA expression of CD31 and VE-cadherin (VE-cad) was detected in all populations. **(E)** There were no significant differences in the expression ratio of VE-cad to β-actin among all cell populations. The expression ratio of CD31 to β-actin was significantly greater in the CD34+ and CD146+ cell populations than in the CD34−CD146− cell population. $^{**}P < 0.01$, $^{*}P < 0.05$. Color images available online at www.liebertonline.com/scd

(ie, pericytes and smooth muscle cells) [44,45]. Similarly, vascular pericytes with CD146 expression have been suggested to arise from CD34+ cells [26]. In addition to these reports, Zengin et al. have recently reported the existence of EPCs and stem cells in a distinct zone between the smooth muscle and the adventitial layer of the human adult vascular wall, which are capable of differentiating into mature endothelial cells and hematopoietic and local immune cells, such as macrophages [27]. Considering these previous reports, it was hypothesized that CD34+ cells could be isolated from the ACL at the site of rupture, which may have similar characteristics to the MSCs described over the last decade [46] and could possibly provide an attractive cell source for tissue repair and regeneration. When cultured, the CD34+ cells lost their expression of CD34 and expressed several makers of MSCs, including CD146, CD44, CD90, and CD73, and they rapidly proliferated (dramatically increased PD times) and were found to be multipotent.

Using H&E staining and immunohistochemical α-SMA staining, we confirmed that the septum region of the ACL and the rupture sites of injured ACLs were richly vascularized when compared with the midsubstance region. Using immunohistochemistry and flow cytometry analysis, we confirmed that CD34+ and CD146+ cells, which demonstrated multilineage differentiation potential, are recruited to the site of rupture and that there are significantly more of these cell types in this area when compared with the midsubstance region. These findings suggest that the rupture site has a rich supply of vascular stem cells that could assist in the intrinsic healing of the ACL. In 48 cases of ruptured ACL healing patterns that were observed by Crain et al., they reported that ruptured ACL remnants were adhering to the

PCL in 38% of the cases, the roof of the notch in 8% of the cases, and the lateral wall of the notch or medial aspect of the lateral femoral condyle in 12% of the cases [47]. These healing patterns could be caused by the instability of the ACL at the rupture site in the synovial fluid, which indicates that applying appropriate primary sutures in the acute phase after injury may be an ideal therapeutic strategy. Based on these latter findings, it is reasonable to posit that there is a rich population of vascular-derived cells present at the ACL rupture site, which could relate to the reason why these reports show spontaneous ACL healing with primary sutures [19–22].

However, the primary suture technique for repairing the ACL tissues may be limited to acute or sub-acute cases because of the ligaments shortening and shrinking during unstable conditions in the synovial fluid. Therefore, recent advances in tissue engineering suggest that suture repair and healing of the ACL may be feasible if a biologic boost is provided at the ligamentous gap using a tissue-engineered scaffold. Murray et al. reported the usefulness of implanting collagen-platelet rich plasma scaffolds for histological and biomechanical ACL healing without reconstruction in animal models [15,48,49]. They used collagen-platelet hydrogels to stimulate healing in a central defect model of canine ACL injury and a complete transection model of a porcine ACL, resulting in significant improvements in histological and biomechanical healing compared with the controls. From the view point of our study, as they reported, scaffolds may be beneficial and necessary for fixation of the ligament and recruitment of cells to heal a complete rupture of the ACL.

Our study may also provide therapeutic options for tendon–bone healing in the ACL reconstruction of the knee. The tissues or cells from the rupture site could be valuable when performing autografts or allografts of the ligament. Similarly, there are some reports showing ACL cells with MSC-like characteristics [23,24]; however, compared with these reports the current study focused on novel vascular cell populations that express the markers CD34 and CD146, which demonstrated a propensity for multilineage differentiation and the potential to be highly expanded. In addition, our findings revealed that tissues at the ACL rupture site, where vascularity is rich, possess an abundant number of stem cells when compared with the mid-substance region of the ligament. On the other hand, reports have shown the contribution and therapeutic potential of MSCs for ligament healing or tendon–bone repair [1,50–52]. Lim and Soon et al. performed bilateral ACL reconstruction in an animal model using grafts coated with MSCs suspended in fibrin glue [50,51]. MSC-treated grafts showed more type II collagen staining at the tendon–bone interface and higher biomechanical strength when compared with fibrin glue-coated grafts with MSCs. Compared with bone marrow MSCs, the ACL cells can be derived from the rupture site of the injured ACL and have the advantage of being easily harvested during arthroscopic examination, which can be performed at the same time as the primary surgery without performing any additional invasive procedures. To confirm the potential therapeutic efficacy of utilizing ruptured tissues or cells for tendon–bone healing, further investigation using an in vivo animal model is required.

Especially important for ligament healing and tendon–bone repair would be for the cells to have the ability to differentiate into osteogenic and endothelial cell lineages. As proof of principle in our study we demonstrated that the vascular stem cells in the ruptured ACL tissue can differentiate into osteoblasts and endothelial cells and also had the ability to differentiate into chondrogenic and adipogenic lineages. There are some reports concerning osteogenesis and angiogenesis/vasculogenesis for ligament and tendon–bone healing. To accelerate osteogenesis and/or angiogenesis for tendon–bone healing, VEGF, granulocyte colony-stimulating factor (G-CSF), TGF-β, BMP2, and BMP7 have recently received attention for their therapeutic potentials (BMP2), and BMP7 have recently received attention for their therapeutic potential [53–57]. On the other hand, Tei et al. reported that human G-CSF mobilized peripheral blood CD34+ cells, which could contribute to ligament healing via their endothelial differentiation (vasculogenesis) capacity and an enhancement of intrinsic angiogenesis by VEGF secretion, in an immunodeficient rat model [58]. In addition, their group also showed that peripheral blood CD34+ cells could differentiate into osteoblasts as well as endothelial cells in a fracture model [59,60]. Compared with their study, the ACL ruptured tissue was shown to contain higher percentages of CD34+ cells (46%) than the peripheral blood (1%) [59], suggesting that the ruptured ACL could be a richer CD34+ cell source than the peripheral blood.

In the current study, there are some limitations. Only relatively acute samples ranging from 3 to 8 weeks postinjury were investigated. Similarly, we selected only young patients from 17 to 29 years old for this study and future studies should compare differential cellular characteristics, including differences in gender, age, and time postinjury. In addition, our study lacked in vivo animal studies, which are important for demonstrating the efficacy of using these cells to actually aid in the repair of ACL injuries.

In conclusion, our results demonstrated that ACL-derived CD34+ cells isolated at the site of ACL rupture, which may originate from the septum, exhibited stem cell characteristics and may contribute to ligament or tendon–bone healing and regeneration. The present findings provide potentially important clinical insights for novel regenerative clinical therapies aimed at enhancing ACL repair and regeneration after injury.

Acknowledgments

The authors are grateful for the technical and scientific advice provided by Jessica Tebbets and Bo Zheng and for the editorial assistance of James Cummins in preparing this article. We are also grateful to Lindsay Mock MT, Tissue Bank Manager of the University of Pittsburgh. This work was supported in part by the Henry J. Mankin Endowed Chair at the University of Pittsburgh and the William F. and Jean W. Donaldson Endowed Chair at the Children's Hospital of Pittsburgh.

Author Disclosure Statement

Johnny Huard has received remuneration as a consultant and has also received royalties from Cook Myosite, Inc. The authors have no conflicts of interest about the present study.

References

1. Agung M, M Ochi, S Yanada, N Adachi, Y Izuta, T Yamasaki and K Toda. (2006). Mobilization of bone marrow-derived mesenchymal stem cells into the injured tissues after

intraarticular injection and their contribution to tissue regeneration. Knee Surg Sports Traumatol Arthrosc 14:1307–1314.
2. Griffin LY, J Agel, MJ Albohm, EA Arendt, RW Dick, WE Garrett, JG Garrick, TE Hewett, L Huston, et al. (2000). Noncontact anterior cruciate ligament injuries: risk factors and prevention strategies. J Am Acad Orthop Surg 8:141–150.
3. Girgis FG, JL Marshall and A Monajem. (1975). The cruciate ligaments of the knee joint. Anatomical, functional and experimental analysis. Clin Orthop Relat Res (106):216–231.
4. Harner CD, GH Baek, TM Vogrin, GJ Carlin, S Kashiwaguchi and SL Woo. (1999). Quantitative analysis of human cruciate ligament insertions. Arthroscopy 15:741–749.
5. Kurosawa H, K Yamakoshi, K Yasuda and T Sasaki. (1991). Simultaneous measurement of changes in length of the cruciate ligaments during knee motion. Clin Orthop Relat Res (265):233–240.
6. Dienst M, RT Burks and PE Greis. (2002). Anatomy and biomechanics of the anterior cruciate ligament. Orthop Clin North Am 33:605–620, v.
7. Duthon VB, C Barea, S Abrassart, JH Fasel, D Fritschy and J Menetrey. (2006). Anatomy of the anterior cruciate ligament. Knee Surg Sports Traumatol Arthrosc 14:204–213.
8. Ferretti M, EA Levicoff, TA Macpherson, MS Moreland, M Cohen and FH Fu. (2007). The fetal anterior cruciate ligament: an anatomic and histologic study. Arthroscopy 23:278–283.
9. Ballock RT, SL Woo, RM Lyon, JM Hollis and WH Akeson. (1989). Use of patellar tendon autograft for anterior cruciate ligament reconstruction in the rabbit: a long-term histologic and biomechanical study. J Orthop Res 7:474–485.
10. Grana WA, DM Egle, R Mahnken and CW Goodhart. (1994). An analysis of autograft fixation after anterior cruciate ligament reconstruction in a rabbit model. Am J Sports Med 22:344–351.
11. Woo SL, M Inoue, E McGurk-Burleson and MA Gomez. (1987). Treatment of the medial collateral ligament injury. II: Structure and function of canine knees in response to differing treatment regimens. Am J Sports Med 15:22–29.
12. Weiss JA, SL Woo, KJ Ohland, S Horibe and PO Newton. (1991). Evaluation of a new injury model to study medial collateral ligament healing: primary repair versus nonoperative treatment. J Orthop Res 9:516–528.
13. Petrigliano FA, DR McAllister and BM Wu. (2006). Tissue engineering for anterior cruciate ligament reconstruction: a review of current strategies. Arthroscopy 22:441–451.
14. Frank CB and DW Jackson. (1997). The science of reconstruction of the anterior cruciate ligament. J Bone Joint Surg Am 79:1556–1576.
15. Murray MM, SD Martin, TL Martin and M Spector. (2000). Histological changes in the human anterior cruciate ligament after rupture. J Bone Joint Surg Am 82-A:1387–1397.
16. Sandberg R, B Balkfors, B Nilsson and N Westlin. (1987). Operative versus non-operative treatment of recent injuries to the ligaments of the knee. A prospective randomized study. J Bone Joint Surg Am 69:1120–1126.
17. Kurosaka M, S Yoshiya, T Mizuno and K Mizuno. (1998). Spontaneous healing of a tear of the anterior cruciate ligament. A report of two cases. J Bone Joint Surg Am 80:1200–1203.
18. Fujimoto E, Y Sumen, M Ochi and Y Ikuta. (2002). Spontaneous healing of acute anterior cruciate ligament (ACL) injuries—conservative treatment using an extension block soft brace without anterior stabilization. Arch Orthop Trauma Surg 122:212–216.
19. Marshall JL, RF Warren, TL Wickiewicz and B Reider. (1979). The anterior cruciate ligament: a technique of repair and reconstruction. Clin Orthop Relat Res (143):97–106.
20. Marshall JL, RF Warren and TL Wickiewicz. (1982). Primary surgical treatment of anterior cruciate ligament lesions. Am J Sports Med 10:103–107.
21. Strand T, A Molster, M Hordvik and Y Krukhaug. (2005). Long-term follow-up after primary repair of the anterior cruciate ligament: clinical and radiological evaluation 15–23 years postoperatively. Arch Orthop Trauma Surg 125:217–221.
22. Drogset JO, T Grontvedt, OR Robak, A Molster, AT Viset and L Engebretsen. (2006). A sixteen-year follow-up of three operative techniques for the treatment of acute ruptures of the anterior cruciate ligament. J Bone Joint Surg Am 88: 944–952.
23. Lee IC, JH Wang, YT Lee and TH Young. (2007). Development of a useful technique to discriminate anterior cruciate ligament cells and mesenchymal stem cells—the application of cell electrophoresis. J Biomed Mater Res A 82:230–237.
24. Lee SY, M Miwa, Y Sakai, R Kuroda, T Matsumoto, T Iwakura, H Fujioka, M Doita and M Kurosaka. (2007). *In vitro* multipotentiality and characterization of human unfractured traumatic hemarthrosis-derived progenitor cells: a potential cell source for tissue repair. J Cell Physiol 210:561–566.
25. Tavian M, B Zheng, E Oberlin, M Crisan, B Sun, J Huard and B Peault. (2005). The vascular wall as a source of stem cells. Ann N Y Acad Sci 1044:41–50.
26. Howson KM, AC Aplin, M Gelati, G Alessandri, EA Parati and RF Nicosia. (2005). The postnatal rat aorta contains pericyte progenitor cells that form spheroidal colonies in suspension culture. Am J Physiol Cell Physiol 289:C1396–C1407.
27. Zengin E, F Chalajour, UM Gehling, WD Ito, H Treede, H Lauke, J Weil, H Reichenspurner, N Kilic and S Ergun. (2006). Vascular wall resident progenitor cells: a source for postnatal vasculogenesis. Development 133:1543–1551.
28. Crisan M, S Yap, L Casteilla, CW Chen, M Corselli, TS Park, G Andriolo, B Sun, B Zheng, et al. (2008). A perivascular origin for mesenchymal stem cells in multiple human organs. Cell Stem Cell 3:301–313.
29. Zheng B, B Cao, M Crisan, B Sun, G Li, A Logar, S Yap, JB Pollett, L Drowley, et al. (2007). Prospective identification of myogenic endothelial cells in human skeletal muscle. Nat Biotechnol 25:1025–1034.
30. Crisan M, B Deasy, M Gavina, B Zheng, J Huard, L Lazzari and B Peault. (2008). Purification and long-term culture of multipotent progenitor cells affiliated with the walls of human blood vessels: myoendothelial cells and pericytes. Methods Cell Biol 86:295–309.
31. Zheng B, B Cao, G Li and J Huard. (2006). Mouse adipose-derived stem cells undergo multilineage differentiation *in vitro* but primarily osteogenic and chondrogenic differentiation *in vivo*. Tissue Eng 12:1891–1901.
32. Zuk PA, M Zhu, H Mizuno, J Huang, JW Futrell, AJ Katz, P Benhaim, HP Lorenz and MH Hedrick. (2001). Multilineage cells from human adipose tissue: implications for cell-based therapies. Tissue Eng 7:211–228.
33. Barry F, RE Boynton, B Liu and JM Murphy. (2001). Chondrogenic differentiation of mesenchymal stem cells from bone marrow: differentiation-dependent gene expression of matrix components. Exp Cell Res 268:189–200.
34. Johnstone B, TM Hering, AI Caplan, VM Goldberg and JU Yoo. (1998). *In vitro* chondrogenesis of bone marrow-derived mesenchymal progenitor cells. Exp Cell Res 238:265–272.
35. Mackay AM, SC Beck, JM Murphy, FP Barry, CO Chichester and MF Pittenger. (1998). Chondrogenic differentiation of cultured human mesenchymal stem cells from marrow. Tissue Eng 4:415–428.

36. Asahara T, T Murohara, A Sullivan, M Silver, R van der Zee, T Li, B Witzenbichler, G Schatteman and JM Isner. (1997). Isolation of putative progenitor endothelial cells for angiogenesis. Science 275:964–967.
37. Bahlmann FH, K De Groot, JM Spandau, AL Landry, B Hertel, T Duckert, SM Boehm, J Menne, H Haller and D Fliser. (2004). Erythropoietin regulates endothelial progenitor cells. Blood 103:921–926.
38. Ma FX, LY Liu and XM Xiong. (2003). Protective effects of lovastatin on vascular endothelium injured by low density lipoprotein. Acta Pharmacol Sin 24:1027–1032.
39. Soeda S, T Kozako, K Iwata and H Shimeno. (2000). Oversulfated fucoidan inhibits the basic fibroblast growth factor-induced tube formation by human umbilical vein endothelial cells: its possible mechanism of action. Biochim Biophys Acta 1497:127–134.
40. Merida-Velasco JA, I Sanchez-Montesinos, J Espin-Ferra, JR Merida-Velasco, JF Rodriguez-Vazquez and J Jimenez-Collado. (1997). Development of the human knee joint ligaments. Anat Rec 248:259–268.
41. Gardner E and R O'Rahilly. (1968). The early development of the knee joint in staged human embryos. J Anat 102:289–299.
42. Scapinelli R. (1997). Vascular anatomy of the human cruciate ligaments and surrounding structures. Clin Anat 10:151–162.
43. Covas DT, RA Panepucci, AM Fontes, WA Silva, Jr., MD Orellana, MC Freitas, L Neder, AR Santos, LC Peres, MC Jamur and MA Zago. (2008). Multipotent mesenchymal stromal cells obtained from diverse human tissues share functional properties and gene-expression profile with CD146+ perivascular cells and fibroblasts. Exp Hematol 36:642–654.
44. Yeh ET, S Zhang, HD Wu, M Korbling, JT Willerson and Z Estrov. (2003). Transdifferentiation of human peripheral blood CD34+-enriched cell population into cardiomyocytes, endothelial cells, and smooth muscle cells *in vivo*. Circulation 108:2070–2073.
45. Iwasaki H, A Kawamoto, M Ishikawa, A Oyamada, S Nakamori, H Nishimura, K Sadamoto, M Horii, T Matsumoto, et al. (2006). Dose-dependent contribution of CD34-positive cell transplantation to concurrent vasculogenesis and cardiomyogenesis for functional regenerative recovery after myocardial infarction. Circulation 113:1311–1325.
46. Pittenger MF, AM Mackay, SC Beck, RK Jaiswal, R Douglas, JD Mosca, MA Moorman, DW Simonetti, S Craig and DR Marshak. (1999). Multilineage potential of adult human mesenchymal stem cells. Science 284:143–147.
47. Crain EH, DC Fithian, EW Paxton and WF Luetzow. (2005). Variation in anterior cruciate ligament scar pattern: does the scar pattern affect anterior laxity in anterior cruciate ligament-deficient knees? Arthroscopy 21:19–24.
48. Murray MM, KP Spindler, C Devin, BS Snyder, J Muller, M Takahashi, P Ballard, LB Nanney and D Zurakowski. (2006). Use of a collagen-platelet rich plasma scaffold to stimulate healing of a central defect in the canine ACL. J Orthop Res 24:820–830.
49. Murray MM, KP Spindler, P Ballard, TP Welch, D Zurakowski and LB Nanney. (2007). Enhanced histologic repair in a central wound in the anterior cruciate ligament with a collagen-platelet-rich plasma scaffold. J Orthop Res 25:1007–1017.
50. Lim JK, J Hui, L Li, A Thambyah, J Goh and EH Lee. (2004). Enhancement of tendon graft osteointegration using mesenchymal stem cells in a rabbit model of anterior cruciate ligament reconstruction. Arthroscopy 20:899–910.
51. Soon MY, A Hassan, JH Hui, JC Goh and EH Lee. (2007). An analysis of soft tissue allograft anterior cruciate ligament reconstruction in a rabbit model: a short-term study of the use of mesenchymal stem cells to enhance tendon osteointegration. Am J Sports Med 35:962–971.
52. Kanaya A, M Deie, N Adachi, M Nishimori, S Yanada and M Ochi. (2007). Intra-articular injection of mesenchymal stromal cells in partially torn anterior cruciate ligaments in a rat model. Arthroscopy 23:610–617.
53. Yoshikawa T, H Tohyama, T Katsura, E Kondo, Y Kotani, H Matsumoto, Y Toyama and K Yasuda. (2006). Effects of local administration of vascular endothelial growth factor on mechanical characteristics of the semitendinosus tendon graft after anterior cruciate ligament reconstruction in sheep. Am J Sports Med 34:1918–1925.
54. Yasuda K, F Tomita, S Yamazaki, A Minami and H Tohyama. (2004). The effect of growth factors on biomechanical properties of the bone-patellar tendon-bone graft after anterior cruciate ligament reconstruction: a canine model study. Am J Sports Med 32:870–880.
55. Sasaki K, R Kuroda, K Ishida, S Kubo, T Matsumoto, Y Mifune, K Kinoshita, K Tei, T Akisue, Y Tabata and M Kurosaka. (2008). Enhancement of tendon-bone osteointegration of anterior cruciate ligament graft using granulocyte colony-stimulating factor. Am J Sports Med 36:1519–1527.
56. Martinek V, C Latterman, A Usas, S Abramowitch, SL Woo, FH Fu and J Huard. (2002). Enhancement of tendon-bone integration of anterior cruciate ligament grafts with bone morphogenetic protein-2 gene transfer: a histological and biomechanical study. J Bone Joint Surg Am 84-A:1123–1131.
57. Mihelic R, M Pecina, M Jelic, S Zoricic, V Kusec, P Simic, D Bobinac, B Lah, D Legovic and S Vukicevic. (2004). Bone morphogenetic protein-7 (osteogenic protein-1) promotes tendon graft integration in anterior cruciate ligament reconstruction in sheep. Am J Sports Med 32:1619–1625.
58. Tei K, T Matsumoto, Y Mifune, K Ishida, K Sasaki, T Shoji, S Kubo, A Kawamoto, T Asahara, M Kurosaka and R Kuroda. (2008). Administrations of peripheral blood CD34-positive cells contribute to medial collateral ligament healing via vasculogenesis. Stem Cells 26:819–830.
59. Matsumoto T, A Kawamoto, R Kuroda, M Ishikawa, Y Mifune, H Iwasaki, M Miwa, M Horii, S Hayashi, et al. (2006). Therapeutic potential of vasculogenesis and osteogenesis promoted by peripheral blood CD34-positive cells for functional bone healing. Am J Pathol 169:1440–1457.
60. Mifune Y, T Matsumoto, A Kawamoto, R Kuroda, T Shoji, H Iwasaki, SM Kwon, M Miwa, M Kurosaka and T Asahara. (2008). Local delivery of granulocyte colony stimulating factor-mobilized CD34-positive progenitor cells using bioscaffold for modality of unhealing bone fracture. Stem Cells 26:1395–1405.

Address correspondence to:
Dr. Johnny Huard
Stem Cell Research Center
University of Pittsburgh
450 Technology Drive
2 Bridgeside Point Suite 206
Pittsburgh, PA 15219

E-mail: jhuard@pitt.edu

Received for publication November 19, 2010
Accepted after revision June 28, 2011
Prepublished on Liebert Instant Online July 6, 2011